IEEE Access
Multidisciplinary | Rapid Review | Open Access Journal

Received 30 April 2023, accepted 28 May 2023, date of publication 23 June 2023, date of current version 7 July 2023.

Digital Object Identifier 10.1109/ACCESS.2023.3289160

RESEARCH ARTICLE

Loss Minimization for Bipolar DC Distribution Grid Considering Probabilistic EV Charging Load Using Load Balancing Method

GUNTINAN SAKULPHAISAN, (Graduate Student Member, IEEE), AND KEERATI CHAYAKULKHEEREE, (Senior Member, IEEE)

School of Electrical Engineering, Institute of Engineering, Suranaree University of Technology, Nakhon Ratchasima 30000, Thailand

Corresponding author: Keerati Chayakulkheeree (keerati.ch@sut.ac.th)

This work was supported by the Suranaree University of Technology.

ABSTRACT This paper proposes a novel method for power loss minimization and voltage unbalance mitigation in bipolar DC distribution grid (DCDG) considering probabilistic electric vehicle (EV) charging load. In the proposed method, a power flow analysis for the bipolar DCDG is performed by G-matrix and Gauss's iteration methods. The Monte Carlo Simulation (MCS) is used to evaluate the impact of EV charging load demand in probabilistic manner. To reduce the impact of the voltage unbalance problem and minimize power loss of the system, particle swarm optimization (PSO) is employed to search for an optimal load connection type that can minimize voltage unbalance factor (VUF) and total power loss. The proposed method was tested with 21-bus DC bipolar system with several cases to verify the potential of the method. The results shown that the proposed method can successfully minimize total power loss and reduce the VUF of the system with probabilistic EV charging load consideration. Therefore, the proposed methodology can be useful for enhancing DCDG operation and mitigating the impact of EV charging.

INDEX TERMS EV charging load, load balancing method, dc power flow, bipolar DC distribution grid.

I. INTRODUCTION

In 1883, a DC distribution system was proposed by Edison for lighting system [1]. Nowadays, the increment of distribution energy resource (DERs) penetration stimulates the interest of DC distribution grid (DCDG). Examples of DCDG are data center and telecommunication systems, which use 48 V_{dc} [2]. As widely known, DCDG has many advantages over AC distribution system. Meanwhile, DCDG has many limitations such as difficulties on high-range voltage levels changing and large DC power generation. A load level increasing in DCDG will cause of voltage drop and high-power loss so the system with high voltage level usually provides better system efficiency and reliability. A voltage level step up or step down of DC voltage need DC – DC converter that have low voltage changing ratio when compare with AC distribution system. The AC distribution system uses transformer to change voltage level which have high voltage changing ratio. For the reason, the AC distribution system technology development becomes popular than DC distribution technology from the past to the present. Three key benefits of home DC power systems over AC systems are as follow: 1. high efficiency, 2. high power quality and 3. not require a synchronization.

Most of present households' appliance use DC power for their internal circuit. Therefore, the household appliances in DC distribution are not require AC – DC converter. In case of electric vehicles (EVs) charging pile, the power loss of power converter stage can be reduced.

In DC systems, the majority of the power quality concerns, that are prevalent in the AC power system, can be easier prevented. Home equipment powered by DC are not experience frequency variation and rarely facing for voltage swell and voltage sag. Additionally, compared to AC microgrids, the cooperative control of PV, wind turbines, and ESS in the DC system is simpler due to the DC power system does not need synchronization feature for distributed generation [3].

The associate editor coordinating the review of this manuscript and approving it for publication was S. K. Panda.

Moreover, a distribution system is facing an emerging high penetration of electric vehicles (EVs) that can extremely increase in load demand leading to effects on stability and security of distribution system [4]. Aforementioned, a load management strategy such as load leveling, load filling or load shifting can reduce an impact of load charging demand by transfer load demand from peak-hours to off-peak hours. On the other hands, a battery of EV can be acted as moveable energy storage device that can charge electricity from grid during off-peak hours and then discharge to grid during peak-hours [5]. Generally, a peak charging time of EV is in the evening and lessen charging load in the morning. A charging load demand evaluation was present in [6] based on Monte Carlo to model a large scale of EV charging demand. The load demand evaluation can be used to limit charging power at charging station via operator or used to manage charging power level of smart charging station for manage load charging demand based on charger connecting time and disconnection time [7], [8], [9].

This paper, therefore, proposes the load balancing method for power loss minimization in bipolar DCDG, considering probabilistic EV charging load. In the proposed method, the particle swarm optimization (PSO) is used to determine the optimal connection for the load at each bus. Meanwhile, the Monte Carlo Simulation (MCS) is used to represent the probabilistic EV charging load in the system.

Aforementioned, the paper was separated into six sections as follow: Section I is the introduction on a DCDG and the influence of EV on distribution system. Next, Section II addresses the overview of voltage level in DCDG including characteristics of unipolar and bipolar DC distribution system. The bus topology of DCDG is illustrated in Section III. Section IV presents bipolar DC power flow calculation. After that, Section V presents a load balancing method which is used to obtain the optimal connection type of load in bipolar DCDG with EV charging station to minimize the power loss of the system. The probabilistic EV charging load model is addressed in Section VI. Section VII presents a simulation result on 21-bus bipolar DC distribution system which comprises of five study cases. Lastly, conclusion is given in section VIII

II. OVERVIEW OF DCDG

The DCDG voltage level is one of main challenges for DCDG voltage standardization. The difference voltage level offer opportunity for a group of users to choose suitable voltage for loads such as residential, commercial and industrial load [10]. Fortunately, the power electronic technology development can bring a new opportunity for DC power distribution.

In case of residential nano grid, A 48 V_{DC} is preferred to interface renewable energy resource to load. However a limitation of 48 VDC is a transmission radius limit in distribution system with multiple households [11].

The primary problem of DC power distribution is voltage level selection of the distribution system. Many standards such as IEC 60038 or IEEE Standard 1709-2010 design to cover field of automotive, marine, computer electronic and aerospace power system that have a specific DC low voltage range, but do not cover a field of distribution system. The medium voltage and low voltage DC (LVDC) distribution voltage guidelines are being developed by China which the desired value of DC voltage level for low voltage distribution 1000V,600V, 440V, 400V, 336V, 240V and 220V [12].

Meanwhile, the voltage level of the LVDC distribution system testbed used by the CIRED workshop is ±750V. Therefore, 750V is a one of popular choices for the residential DC power systems [13]. A highest LVDC is 1.5 kV for distribution system that is a 750 V bipolar distribution grid that offer two voltage level options for residential load that comprise of ± 750 V and ± 1.5 kV with DC converter as an interface to match the voltage levels for households' loads [14].

III. BUS TOPOLOGY OF DCDG

A DCDG comprises of 1.) DC bus 2.) AC/DC converter, and 3.) load. Normally, a DC bus is used to connect to main grid via AC/DC converter to convert AC voltage to DC voltage and serve power to the load. To compare a loss characteristic of AC distribution system with DCDG, DCDG is a good solution to reduce power loss by reduce amount of power conversion. The system efficiency, cost, and system size are the advantage of DCDG. Additionally, DCDG has high stability owing to the absence of reactive power and is more suitable for distributed energy resources (DERs) integration [15]. Moreover, DCDG can transmit power with two configurations which are unipolar and bipolar systems, that offer difference system abilities such as available voltage level, reliability and power quality.

A. DC UNIPOLAR BUS TOPOLOGY

A DC unipolar system bus topology like a single-phase AC power system that has only two wires for distribute power to load. In case of DC unipolar bus, the wires are called positive wire and negative wire which a source and loads are connected between the wires, as shown in FIGURE 1. The energy is transferred through the DC bus with single voltage level. So, the DC bus voltage level choosing is important in this system. The system capability depends on voltage level which the high voltage level can increase power transmission system capability, but the DC-DC converter is needed reduce the user voltage level for safety uses. The suitable voltage level selection can avoid large number of DC – DC converter deployment. This topology is practical for off-grid homes in isolated rural locations without utility grid infrastructure. DC unipolar system is simple to implement with symmetry between the pole. On the other hand, a single fault can be led to shut down the system and does not offer different voltage levels option to the users [16], [17].

B. DC BIPOLAR BUS TOPOLOGY

A DC bipolar bus topology has some advantage over DC unipolar bus topology. Its structure is similar to a three-phase

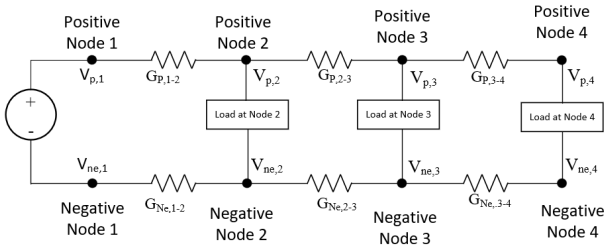

FIGURE 1. Typical DC unipolar bus topology.

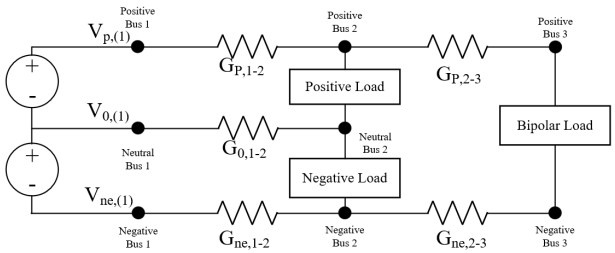

FIGURE 2. Typical DC bipolar bus topology.

AC power system with three wires for transferring energy to load. The wires are called positive line, negative line and neutral line, as shown in FIGURE 2. The topology offers three voltage levels option which consisted of $+V_{DC}$, $-V_{DC}$ and $2V_{DC}$. Under a fault condition, the load at fault bus in bipolar DC bus topology can be transfer to other pole at same bus. Therefore, the reliability, power quality and availability of the system during fault condition are better than unipolar DC bus topology. A difference voltage levels option offers a flexibility to consumer, but can result in the system unbalance condition. The unbalance condition can increase neutral current flow and lead to increase in overall system power loss. So, the system requires a voltage balancer or load balance strategy to prevent unbalance condition [18].

IV. BIPOLAR DC POWERFLOW CALCULATION

FIGURE 3 represents the components of bipolar DC power system which comprises of DC substation, transmission line and load (positive load, negative load and bipolar load). This paper uses the method called G-Matrix Method (GMM) for DC load flow analysis [19]. To calculate a power flow model, the network component comprises of two type of bus which are source and load buses. The source bus is replaced by slack bus which represent by index '1' and load bus starts at index '2' to index 'n'. The conductance of every transmission line between bus is donated by Gij which index 'i' to index 'j' are starting bus and ending bus of conductance in [G]. A bipolar DC network have three cables. So, in [G] have to consists of G+/0/- that represents cable conductance of positive neutral and negative cable from bus i to bus j. V+/0/- is a positive, neutral and negative voltage at bus i while Ip/n/b represent load current at each pole. Ip and In are called unipolar load that draw load current from positive pole or negative pole and return to substation via neutral pole. Ib represent a bipolar

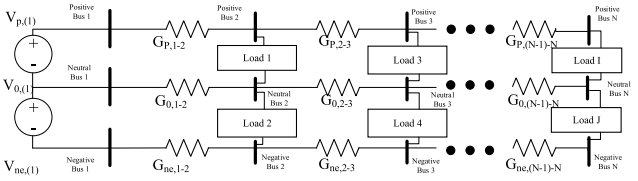

FIGURE 3. Component of DC power system.

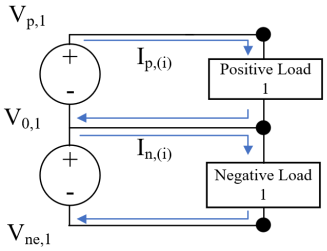

FIGURE 4. Unipolar connection in bipolar DC bus topology.

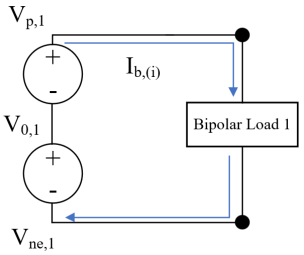

FIGURE 5. Current flow in Bipolar connection of bipolar DC bus topology.

load that draws load current from positive pole and return to substation via negative pole. So, the single line diagram is modeled by nodal analysis that represent the relationship of unipolar and bipolar load current. The direction of loads currents is shown in FIGURE 4 and FIGURE 5.

A load voltage drop can be calculated by consider the difference of voltage between connection pole as,

$$V_{p,i} = V_{+,i} - V_{0,i} \text{ and} \tag{1}$$

$$V_{n,i} = V_{0,i} - V_{-,i}. \tag{2}$$

where $V_{p,i}$ represents voltage drop of unipolar load at bus i when refer positive pole and neutral pole. $V_{+,i}$, $V_{-,i}$ and $V_{0,i}$ represent voltage at positive pole, voltage at negative pole and neutral pole at bus i, respectively. Therfore, $V_{+,i}$ and $V_{-,i}$ represent voltage drop of unipolar load at bus i when refer to the neutral pole and negative pole. The sign of $V_{-,i}$ must be negative to present a direction of current flow from neutral pole to negative pole that represent a current must flow from high voltage to low voltage.

The voltage drops at each bus from Equations (1)-(2) are used to calculate currents at each bus by using Equations (3)-(4) as,

$$I_{p,\mathrm{i}} = \frac{P_{p,\mathrm{i}}}{V_{p,\mathrm{i}}} \text{ and} \tag{3}$$

$$I_{n,\mathrm{i}} = \frac{P_{n,\mathrm{i}}}{V_{n,\mathrm{i}}}. \tag{4}$$

where $I_{p,i}$ and $I_{n,i}$ represent a positive pole load and negative pole load at bus i and $P_{p,i}$ and $P_{n,i}$ represent unipolar connection load at bus i that refer to positive and negative load connections.

In case of bipolar load connection, the load connects between positive pole and negative pole, as shown in FIGURE 5. The load nominal voltage is therefore, $2V_{DC}$. The bipolar load voltage drop can be calculated by Equation (5),

$$V_{b,i} = V_{+,\mathrm{i}} - V_{-,\mathrm{i}}. \tag{5}$$

where $V_{b,\mathrm{i}}$, $V_{+,i}$ and $V_{-,i}$ are bipolar load voltage drop, positive voltage pole and negative voltage pole. So, the bipolar load current can be calculated by Equation (6),

$$I_{b,\mathrm{i}} = \frac{P_{b,\mathrm{i}}}{V_{b,i}}. \tag{6}$$

where $I_{b,i}$ is the bipolar load current at bus i. $P_{b,i}$ and $V_{b,i}$ are bipolar load capacity at bus i and bipolar load voltage drop at bus i, respectively. The substation can be replaced as a slack bus which can be assumed the nominal voltages at 1 p.u., 0 p.u., and – 1 p.u., for positive bus, neutral bus and negative bus, respectively. The transmission lines are modeled by conductance between buses. So, the power flow equation of system can be calculated by.

$$[\mathbf{I}] = [\mathbf{G}]\,[\mathbf{V}], \tag{7}$$

or

$$\begin{bmatrix} \mathbf{I_p} \\ \mathbf{I}_0 \\ \mathbf{I_n} \end{bmatrix} = \begin{bmatrix} \mathbf{G_p} & 0 & 0 \\ 0 & \mathbf{G}_0 & 0 \\ 0 & 0 & \mathbf{G_n} \end{bmatrix} \begin{bmatrix} \mathbf{V_p} \\ \mathbf{V}_0 \\ \mathbf{V_n} \end{bmatrix}, \tag{8}$$

where

$$\mathbf{V_p} = \begin{bmatrix} \mathbf{V_{p,1}} & \mathbf{V_{p,2}} & \cdots & \mathbf{V_{p,N}} \end{bmatrix}^{\mathbf{T}}, \tag{9}$$

$$\mathbf{V}_0 = \begin{bmatrix} \mathbf{V}_{0,1} & \mathbf{V}_{0,2} & \cdots & \mathbf{V_{0,N}} \end{bmatrix}^{\mathbf{T}}, \tag{10}$$

$$\mathbf{V_n} = \begin{bmatrix} \mathbf{V_{n,1}} & \mathbf{V_{n,2}} & \cdots & \mathbf{V_{n,N}} \end{bmatrix}^{\mathbf{T}}, \tag{11}$$

$$\mathbf{I_p} = \begin{bmatrix} \mathbf{I_{p,1}}+\mathbf{I_{b,1}} & \mathbf{I_{p,2}}+\mathbf{I_{b,2}} & \cdots & \mathbf{I_{p,N}}+\mathbf{I_{b,N}} \end{bmatrix}^{T}, \tag{12}$$

$$\mathbf{I}_0 = \begin{bmatrix} \mathbf{I}_{0,1} & \mathbf{I}_{0,2} & \cdots & \mathbf{I_{0,N}} \end{bmatrix}^{T}, \tag{13}$$

$$\mathbf{I_n} = \begin{bmatrix} \mathbf{I_{n,1}}+\mathbf{I_{b,1}} & \mathbf{I_{n,2}}+\mathbf{I_{b,2}} & \cdots & \mathbf{I_{n,N}}+\mathbf{I_{b,N}} \end{bmatrix}^{T}, \tag{14}$$

$$\mathbf{G_p} = \begin{bmatrix} \sum\limits_{i\leftrightarrow 1} G_{p,1i} & -G_{p,12} & \cdots & -G_{p,1N} \\ -G_{p,21} & \sum\limits_{i\leftrightarrow 1} G_{p,2i} & -G_{p,23} & -G_{p,2N} \\ \vdots & \vdots & \ddots & \vdots \\ -G_{p,N1} & -G_{p,N2} & \cdots & \sum\limits_{i\leftrightarrow 1} G_{p,NN} \end{bmatrix}, \tag{15}$$

$$\mathbf{G}_0 = \begin{bmatrix} \sum\limits_{i\leftrightarrow 1} G_{0,1i} & -G_{0,12} & \cdots & -G_{0,1N} \\ -G_{0,21} & \sum\limits_{i\leftrightarrow 1} G_{0,2i} & -G_{0,23} & -G_{0,2N} \\ \vdots & \vdots & \ddots & \vdots \\ -G_{0,N1} & -G_{0,N2} & \cdots & \sum\limits_{i\leftrightarrow 1} G_{0,NN} \end{bmatrix}, \tag{16}$$

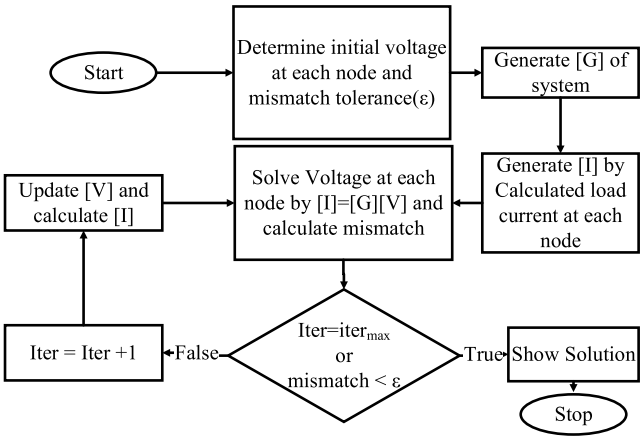

FIGURE 6. Bipolar DC power flow procedure.

$$\mathbf{G}_{ne} = \begin{bmatrix} \sum\limits_{i\leftrightarrow 1} G_{ne,,1i} & -G_{ne,12} & \cdots & -G_{ne,1N} \\ -G_{ne,21} & \sum\limits_{i\leftrightarrow 1} G_{ne,2i} & -G_{ne,23} & -G_{ne,2N} \\ \vdots & \vdots & \ddots & \vdots \\ -G_{ne,N1} & -G_{ne,N2} & \cdots & \sum\limits_{i\leftrightarrow 1} G_{ne,NN} \end{bmatrix}. \tag{17}$$

where **[G]**, **[I]** and **[V]** represent conductance matrix, current matrix and voltage matrix of network, respectively. The symbol "i↔j" donates "i connected to j". So, the power flow calculation can be calculated by replace Equation (9)-Equation (17) in Equation (8) to calculate voltage profile, current flow between buses. The computational procedure is shown in FIGURE 6.

V. PARTICLE SWARM OPTIMIZATION BASED LOAD BALANCING METHOD

In DCDG, the voltage drop between two nodes is depended on the current flow through their interconnecting cables. In the other word, voltage at each bus in DCDG is depended on the distributed load in the grid [20]. So, the main problem of bipolar DCDG is the load unbalance condition, due to the load can be connected to both positive or negative pole, as shown in FIGURE 3. Generally, load unbalance problem is caused by unplanned households' and EV charging loads [21]. This problem increases current flow in neutral wire, leading to increase in overall system power loss. There are several ways to reduce voltage imbalance in LVDC, For example, the voltage balancer. that controls the voltage of the DC/DC converter at point of common coupling (PCC) to compensate voltage drop at each bus. A demand response or load balancing with electrical price is one of alternative methods to reduce load unbalance by using an energy price to control load demand characteristic of DC bipolar distribution grid and reduce power difference between poles [22].

In this paper, particle swarm optimization (PSO) in [23] is used to search an optimal load connection and EV charging load. The objective function (OF) is to minimize total energy

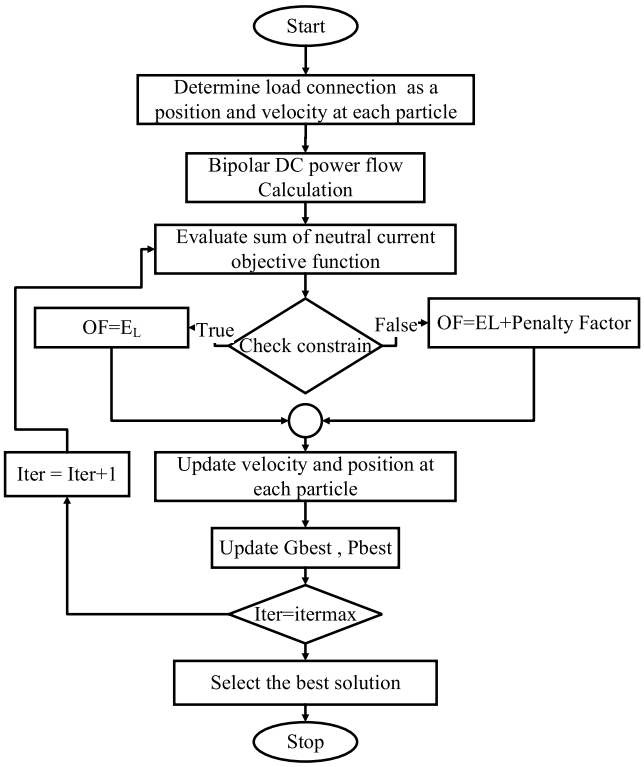

FIGURE 7. PSO based load balancing method procedure.

loss as,

$$Minimize\ E_L = \sum_{t=1}^{48} \left[P_{L,p}(t) + P_{L,0}(t) + P_{L,n}(t)\right], \quad (18)$$

where

$$P_{L,p} = \sum_{i=1}^{n-1} I_{p,(i,j+1)}^2 G_{p(i,i+1)}, \quad (19)$$

$$P_{L,0} = \sum_{i=1}^{n-1} I_{0,(i,i+1)}^2 G_{0(i,i+1)}, \quad (20)$$

$$P_{L,n} = \sum_{i=1}^{n-1} I_{n,(i,i+1)}^2 G_{n(i,i+1)}, \quad (21)$$

subject to the constraints

$$V_{\mathrm{p\,min,i}} \le V_{\mathrm{p},i} \le V_{\mathrm{p\,max,i}}, \quad (22)$$

$$V_{\mathrm{0\,min,i}} \le V_{0,i} \le V_{\mathrm{0\,max,i}}, \quad (23)$$

$$V_{\mathrm{p\,min,i}} \le V_{\mathrm{p},i} \le V_{n\,\mathrm{max,i}}, \text{ and} \quad (24)$$

$$\%VUF < \%VUF_{\max} \quad (25)$$

where subscript p, 0 and n represent positive pole, negative pole, and neutral pole, respectively. The computational procedure is shown in FIGURE 7.

VI. PROBABILISTIC EV CHARGING LOAD BASED ON MONTE CARLO SIMULATION

In this paper, the MCS method is used to simulate various factor that affect to EV charging load characteristic, such as charging plug-in time and plug-out time, initial state of charge (SOC), daily travel distance, charging duration and charging type. In the home-charging pattern, the EV owners will plug their car when arrive home after work and remove the plug for travel to work. A probabilistic distribution function (PDF) that represent the charging behavior of EV owner can be expressed as,

$$f_c(t_c) = \begin{cases} \dfrac{1}{\sqrt{2\pi}\sigma_c} \exp\left(-\dfrac{(t_c + 24 - \mu_c)^2}{2\sigma_c^2}\right), \\ \qquad 0 < t_c \le \mu_c - 12 \\ \dfrac{1}{\sqrt{2\pi}\sigma_c} \exp\left(-\dfrac{(t_c - \mu_c)^2}{2\sigma_c^2}\right), \\ \qquad \mu_c - 12 < t_c \le 24 \end{cases}, \quad (26)$$

where t_c, σ_c and μ_c are EV plug-in time, plug-in standard deviation and mean of plug-in time, respectively. The standard deviation and mean of plug-in time are used to generate the sampling probabilistic plug-in time behavior of EV owners.

The PDF that represents the daily travel distance of EV in each day be calculated by,

$$f_d(d) = \frac{1}{\sqrt{2\pi}\sigma_d} \exp\left(-\frac{(d - \mu_d)^2}{2\sigma_d^2}\right), 0 \le d \le D \quad (27)$$

where d is the daily travel distance of the EV. D is the maximum travel distance at the EV. $\sigma_{\mathbf{c}}$, and $\mu_{\mathbf{c}}$ are the standard deviation and mean of the EV travel distance, respectively.

After calculate the daily travel distance, the result is used to calculate the remaining SOC of EV before charging which can be calculated by,

$$SOC_i = 1 - \frac{d_i}{D_i \times \eta_i}. \quad (28)$$

where subscript i denotes the parameters of the i^{th} EV. Whereas, η_i, represents efficiency of the i^{th} EV.

In the daily scheduling process, the scheduling time is divided into 96 time slot which the length of time slot is 15 minutes. So, the arrival time and departure time of each EV can be calculated by,

$$T_{c,i} = \frac{t_{c,i}}{\Delta T}, \quad (29)$$

$$T_{d,i} = \frac{t_{d,i}}{\Delta T}, \text{ and} \quad (30)$$

$$T_{r,i} = T_{c,i} - T_{d,i}. \quad (31)$$

When $t_{c,i}$, $t_{d,i}$, and ΔT are plug-in time, plug-off time and duration of time slot, respectively. $T_{c,i}$, $T_{d,i}$ and $T_{r,i}$ are plug-in time, plug-off time and remaining time based on time slot, respectively.

To calculate charging level index or charging urgency indicator, the arrival time slot and departure time slot are used to

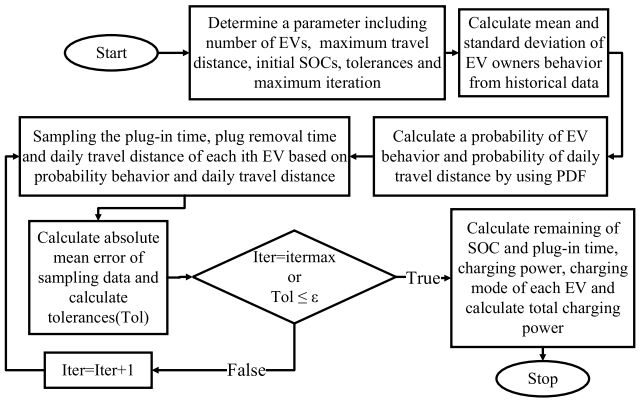

FIGURE 8. MCS based probabilistic EV charging.

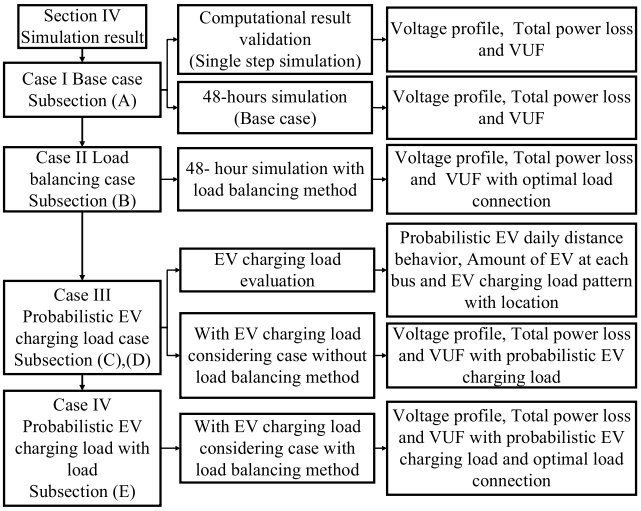

FIGURE 9. Simulation category overview.

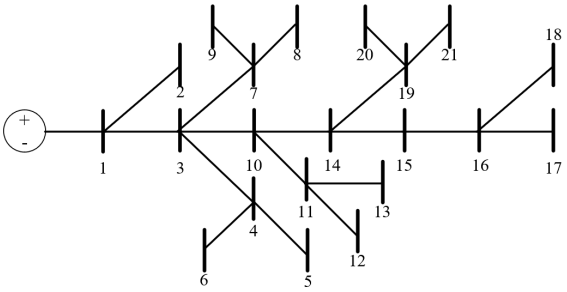

FIGURE 10. IEEE 21 bus case study system.

calculate indicator to manage the charging power level. In this study, the charging urgency indicator is referred to [36] as

$$CUI_i = \left(T_{r,i} \times \Delta T\right) \times P_{EV,i}^{slow} \times \eta_{EV} - \left(SOC_i^{\min} - SOC_i^{con}\right) \times Cap_{EV,i}^{batt}. \quad (32)$$

When CUI_i is charging urgency indicator which is used to choose the charging level of each EV. $P_{EV,i}^{slow}$, $SOC_i^{\min}$, SOC_i^{con}, and $Cap_{EV,i}^{batt}$ are the slow charging power of EVs, the minimum SOC required for the i^{th} EV after charging, the SOC level of the i^{th} EV when connected to charger, and the battery capacity of the i^{th} EV, respectively. If CUI_i is higher than 0, the charging level is slow charging level. In the other hand, the CUI_i is less than 0, the charging level is fast charging level. The procedure of probabilistic EV load model based on MCS is shown in FIGURE 8.

In FIGURE 8, the EV owner behavior comprises of daily travel distance, charging time and unplugging time are presented. The EV owners data is used to calculate mean, standard deviation and PDF to present the likelihood of EV owners' activities.

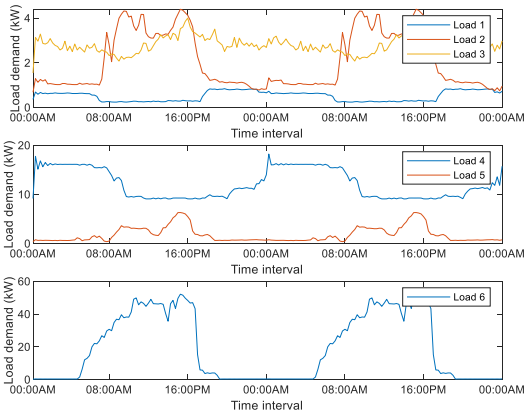

FIGURE 11. 48 hrs. load profile.

TABLE 1. IEEE 21 bus system data.

From bus	To bus	Resistance
1	2	0.053
1	3	0.054
3	4	0.054
4	5	0.063
4	6	0.051
3	7	0.037
7	8	0.079
7	9	0.072
3	10	0.053
10	11	0.038
11	12	0.079
11	13	0.078
10	14	0.083
14	15	0.065
15	16	0.064
16	17	0.074
16	18	0.081
14	19	0.078
19	20	0.084
19	21	0.082

VII. SIMULATION RESULT

The simulation study can be separated into 4 cases including,

Case I : Base case,

Case II : Load balancing case,

Case III : Probabilistic EV charging load case, and

TABLE 2. IEEE 21 load data for validation simulation.

Bus	Positive Pole Load (kW)	Negative Pole Load (kW)	Bipolar Load (kW)
1	0	0	0
2	70	100	0
32	0	0	0
4	36	40	120
5	4	0	0
6	36	0	0
7	0	0	0
8	32	50	0
9	80	0	100
10	0	10	0
11	45	30	0
12	68	70	0
13	10	0	75
14	0	0	0
15	22	30	0
16	23	10	0
17	43	0	60
18	34	60	0
19	9	15	0
20	21	10	50
21	21	20	0

TABLE 3. Load Connection type of base case.

Bus	Positive pole Load	Negative Pole Load	Bipolar Load
1	-	-	-
2	Load 2(A), Load 3(B)	-	-
3	-	-	-
4	-	Load 1(A), Load 5(B)	Load 4
5	-	Load 2(A)	-
6	-	Load 2(A)	-
7	-	-	-
8	Load 1 (A)	Load 2(B)	-
9	Load 2 (A)	-	Load 4
10	-	Load 3 (B)	-
11	-	Load 1 (A), Load 2 (B)	-
12	-	Load 4 (A), Load 5 (B)	-
13	-	-	Load 6
14	-	-	-
15	Load 5 (A)	Load 1 (B)	-
16	Load 5 (A)	Load 3 (B)	-
17	-	Load 5 (A)	Load 6
18	-	Load 2 (A), Load 5 (B)	-
19	-	Load 1 (A), Load 2(B)	-
20	-	Load 1 (A), Load 3(B)	Load 6
21	-	Load 1 (A), Load 2(B)	-

Case IV : Probabilistic EV charging load with load balancing case.

The simulation study comprises of two categories as follow: 1) single step simulation 2) 48-hours simulation. A single step simulation is used to validate computational result and illustrate the load affect to voltage profile via *VUF* and evaluate power loss of the system. A 48-hours simulation is used to simulate ability of load balancing method in cases with and without EV charging load based on MCS. The simulation study overview is shown in FIGURE 9.

The IEEE 21-bus system is used as test system. The system topology is showed in FIGURE 10 and the parameters of the system are shown in TABLE 1 to TABLE 3. In case of 48 hours simulation, the system load profile data are shown in FIGURE 10 with load types in TABLE 3.

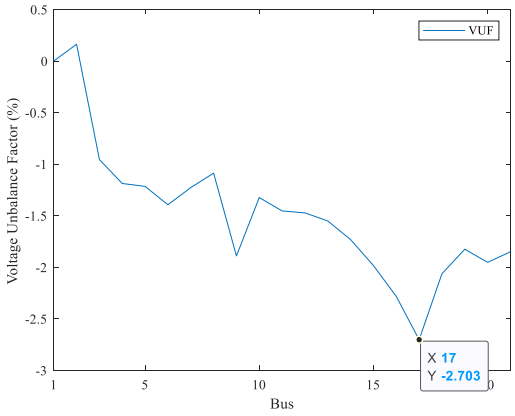

FIGURE 12. Voltage unbalance factor at each bus of base case result.

TABLE 4. Base case simulation result.

Bus	Voltage (V) (simulation)			Voltage (V) (reference)		
	V+	V0	V-	V+	V0	V-
1	1000	0	-1,000	1,000	0	-1,000
2	996.28	-1.62	-994.66	996.28	-1.62	-994.66
3	959.52	9.22	-968.74	959.52	9.22	-968.74
4	951.76	11.37	-963.14	951.76	11.37	-963.14
5	951.50	11.64	-963.14	951.50	11.64	-963.14
6	949.80	13.33	-963.14	949.80	13.33	-963.14
7	953.12	11.77	-964.89	953.12	11.77	-964.89
8	950.43	10.39	-960.82	950.43	10.39	-960.82
9	943.11	17.80	-961.11	943.11	17.10	-961.11
10	936.57	12.49	-949.06	936.57	12.49	-949.06
11	929.93	13.62	-943.55	929.93	13.62	-943.55
12	924.02	13.71	-937.73	924.02	13.71	-937.73
13	925.94	14.48	-940.41	925.94	14.48	-940.41
14	915.16	15.99	-931.15	915.16	15.99	-931.15
15	903.90	18.11	-922.02	903.90	18.11	-922.02
16	894.41	20.66	-915.07	894.41	20.66	-915.66
17	888.26	24.34	-912.60	888.26	24.34	-912.60
18	891.25	18.58	-909.83	891.25	18.58	-909.83
19	908.55	16.74	-925.29	908.55	16.74	-925.29
20	904.26	17.83	-922.09	904.26	17.83	-922.09
21	906.62	16.98	-923.54	906.61	16.93	-923.54
Validation error (%)				<0.01 %		
Total power loss (kW)				95.42		
Maximum VUF (%)				-2.7 (At bus 17)		

A. BASECASE

This subsection presents the result of power flow solving of bipolar DCDG to validate a simulation result with reference [37] and used to compare with other cases for evaluate

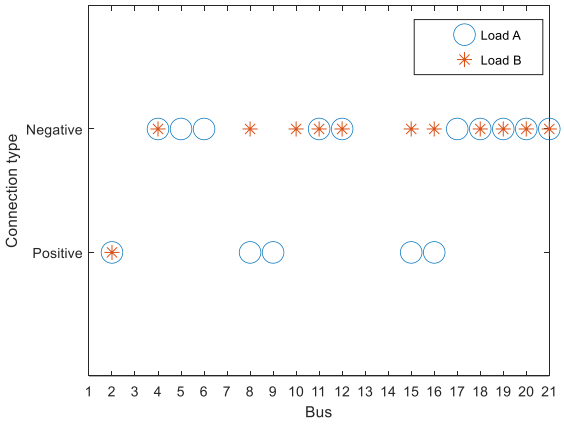

FIGURE 13. Load connection type of base case.

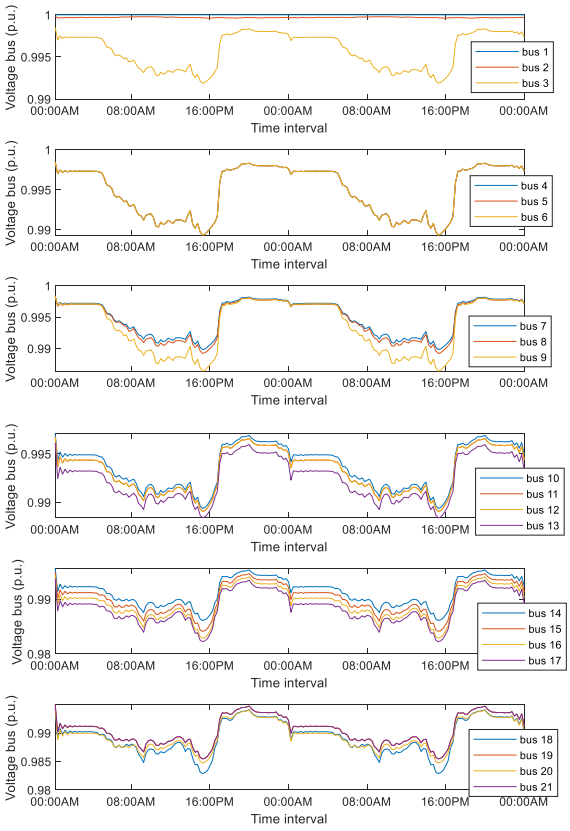

FIGURE 14. Positive voltage profile of base case.

the performance of the proposed method. The simulation result is shown in TABLE 4. FIGURE 12 presents the *VUF*s of the system at all buses.

In TABLE 4, the simulation results including the base case voltage unbalance factor, voltage profile and total loss are addressed. The positive VUF is due to load at negative pole is higher than that of in positive pole in each bus. In the other hand, the negative VUF is due to positive pole load higher than that of in negative pole. The simulation resulted in the highest VUF of -2.7% at bus 17, and total power loss is 95.42 kW with mismatch error less than 0.01 %. FIGURE 13 presents connection type of load A and load B to positive load and negative load, as referred to TABLE 3.

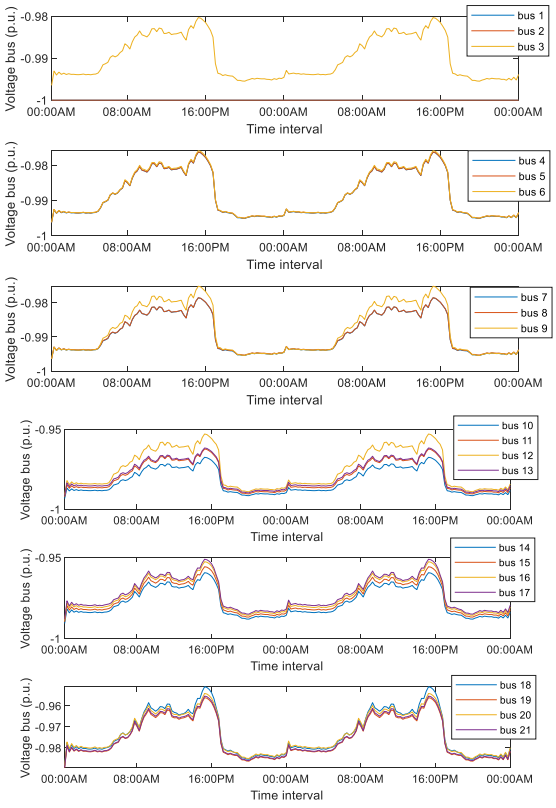

FIGURE 15. (a) Positive voltage profile of base case. (b) Negative voltage profile of base case(cont).

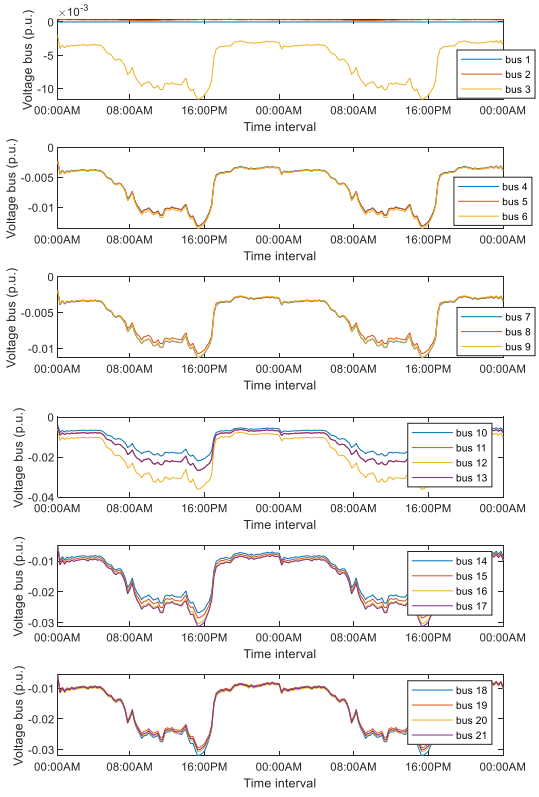

FIGURE 16. Neutral voltage profile of base case.

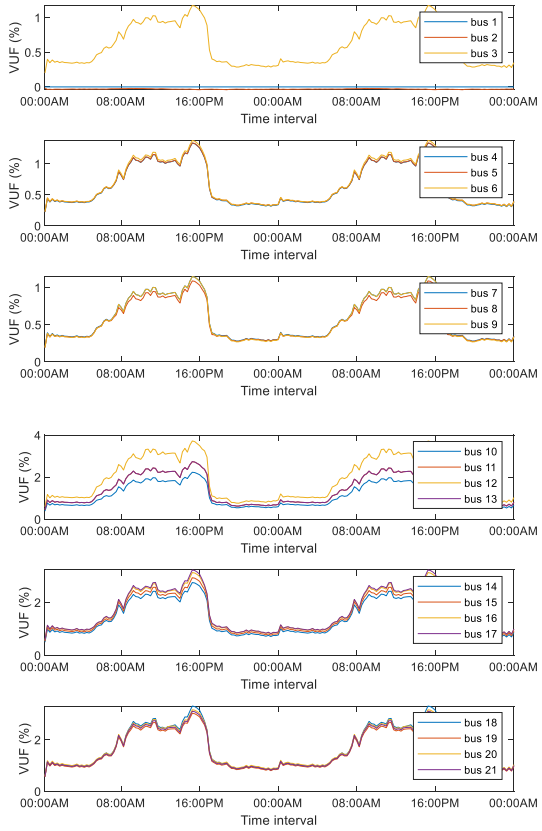

FIGURE 17. 48 hours VUF of base case.

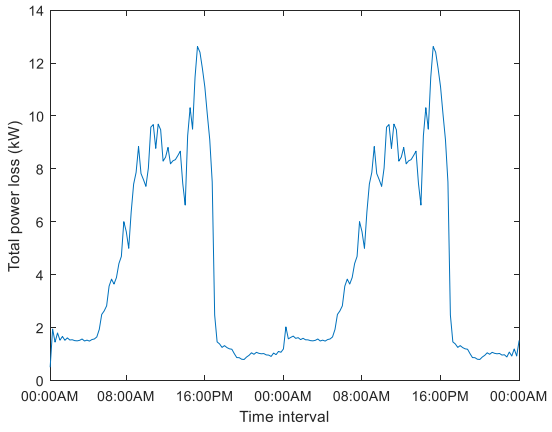

FIGURE 18. Total power loss of base case.

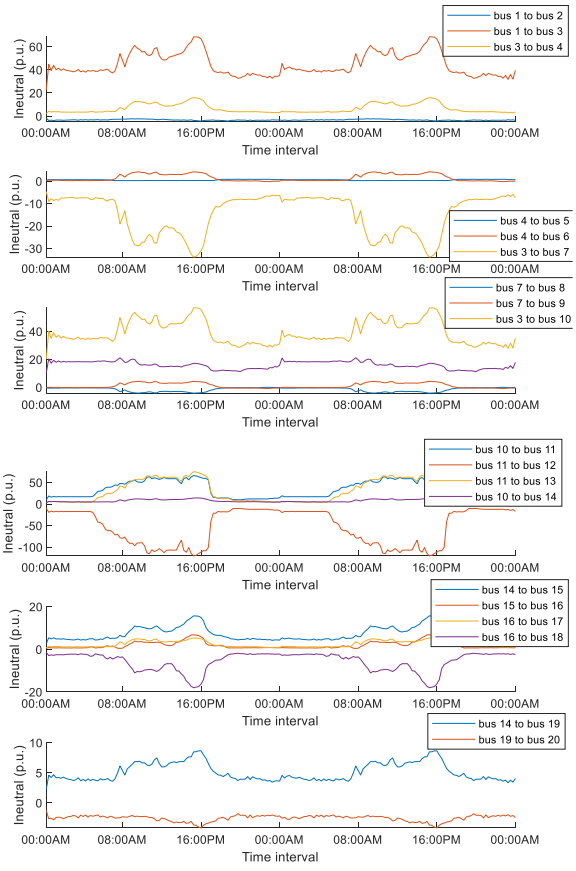

FIGURE 19. Neutral current flow of base case.

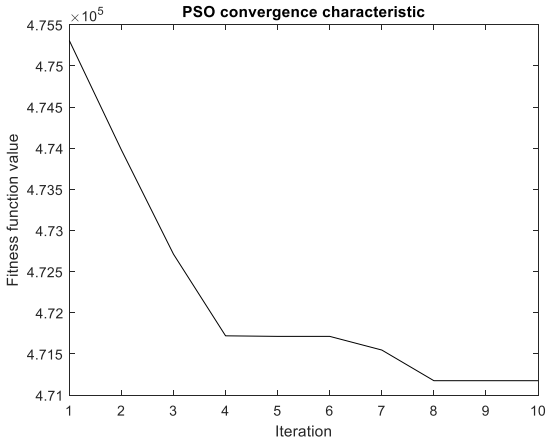

FIGURE 20. PSO convergence characteristic.

FIGURES 14-15 present the positive and negative voltage profile of base case scenario with the load profile in FIGURE 12. The lowest voltage at bus 17 for positive voltage and bus 18 for negative voltage at 15.30 p.m. (timeslot 61). In this case, the load demand at bus 17 includes 6.34 kW at negative pole and 9.26 kW with bipolar connection. Bus 18 was resulted in the lowest negative voltage magnitude. The cause of problem is due to total load demand on negative pole that comprises of 2 load demand, as shown in TABLE 3. The simulation results show that the negative voltage at this bus is -0.950 p.u. and 0.983 p.u. for positive voltage, with 3.34 % of VUF.

FIGURE 17 presents the VUF of the system for 48 hours. the neutral voltage profiles of base case are shown in FIGURE 16. The magnitude of neutral voltage changes in according to VUF at each bus. The neutral voltage in FIGURE 17 is influenced by unbalance load demand at each pole.

FIGURE 18 present the power loss of the system that is varied by the load demand at each time interval. The highest power loss take place at 15.30 p.m. (time slot 61).

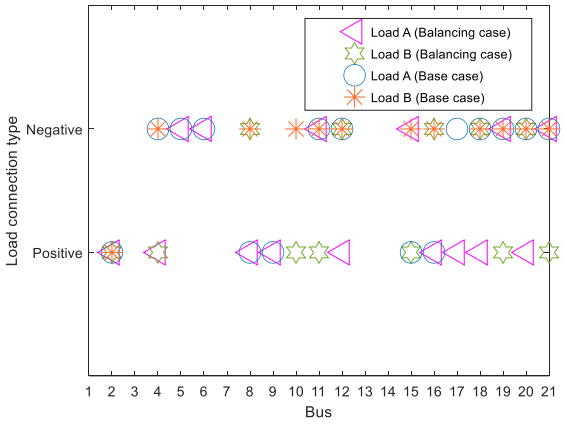

FIGURE 21. Load connection type comparisons of base case and load balancing case.

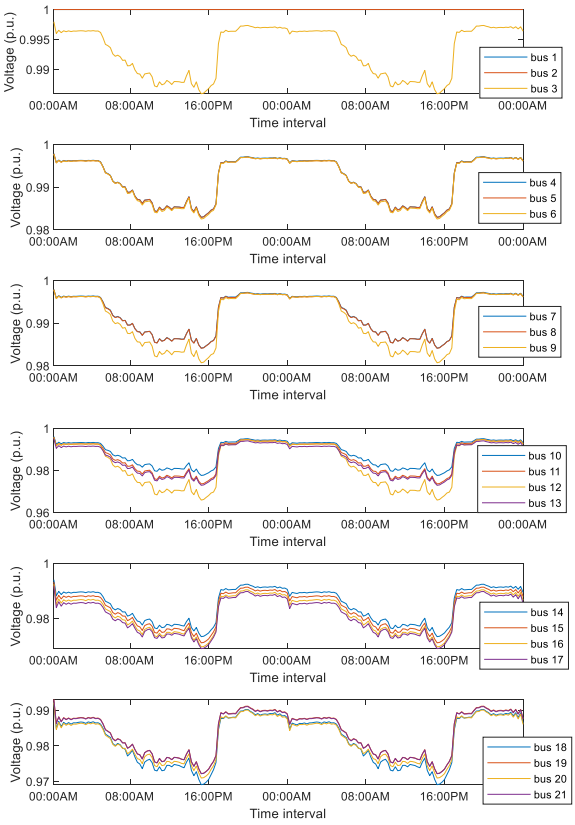

FIGURE 22. Positive voltage profile of load balancing case.

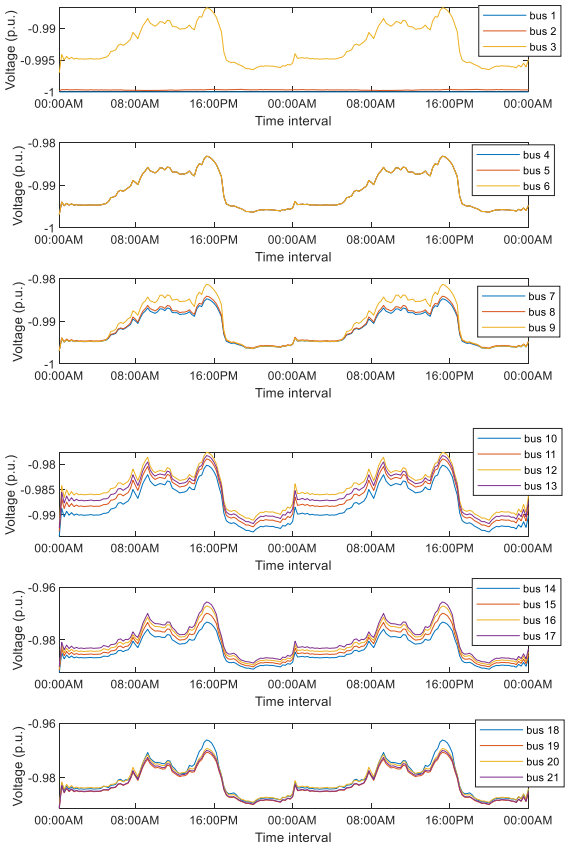

FIGURE 23. Negative voltage profile of load balancing case.

TABLE 5. Particle swarm optimization method parameter.

Variable	Value
Lower bound	1 (Replace positive connection)
Upper bound	2 (Replace positive connection)
Number of variables	42
Maximum inertia weight	0.9
Minimum inertia weight	0.4
Acceleration factor 1	2
Acceleration factor 2	2
Population size	500
Maximum number of iterations	10
Maximum number of runs	5

At 15.30 p.m. the load demand at bus 18 connected at the negative pole only, leading to unbalance voltage at the bus and the total daily loss of entire system is equal to 958.100 kWh. FIGURE 19 present a neutral power flow between buses. The highest neutral current flow take place between bus 1 and bus 3 at 15.30 p.m.

B. LOAD BALANCING CASE (CASE II)

This subsection presents a simulation result of load balancing method with the objective of minimizing power loss of the system using PSO. The proposed concept is for planning phase to find the best connection type of every load that minimize system power loss and VUF. The PSO parameters are shown in TABLE 5. The simulation results including PSO convergence characteristic, load type, power loss and voltage profile are shown in FIGURES 20-25. Note that, the maximum VUF limit constraint used is 3%.

FIGURE 20 presents a convergence of optimization method which the best fitness function value is 471,200 at iteration 8. The result of optimal load connection types is shown in FIGURE 21. The voltage profile and VUF are shown in FIGURES 22 -25.

FIGURE 21 compares the load connection type of balancing case and base case. The objective of load balancing is to

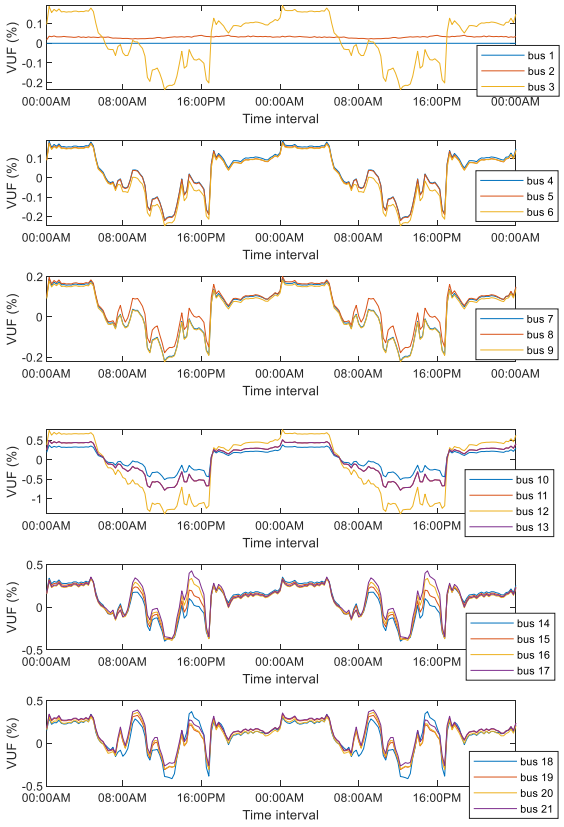

FIGURE 24. Voltage unbalance factor (VUF) of load balancing case.

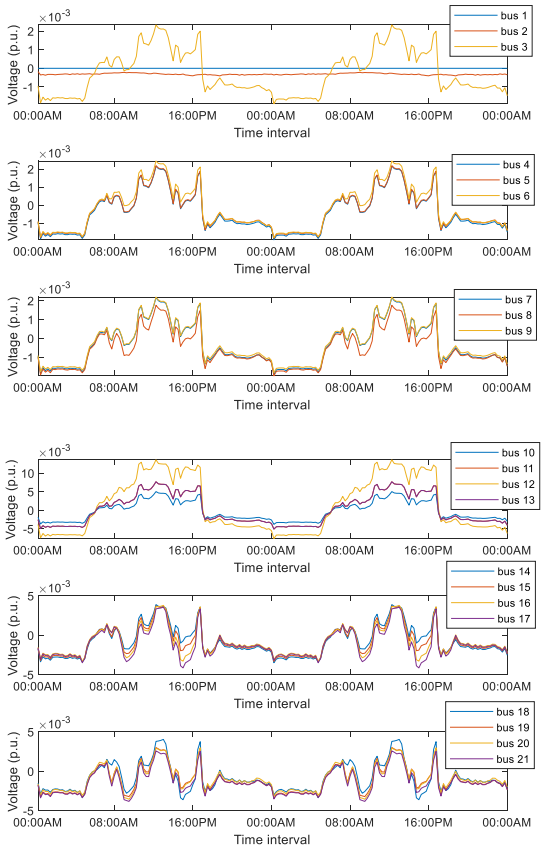

FIGURE 25. Neutral voltage profile of load balancing case.

TABLE 6. Monte carlo simulation condition.

Data	Condition
Number of EV	50
Charger bus	[1,21]
Initial of battery SOC	100 %
Charger plug-in time	Depend on sampling data from PDF
Charger removes time	08.00 AM every day
Iteration	10,000
Tolerance	10^{-5}
Standard deviation of plug-in time	18
Mean of plug-in time	3.3
Standard deviation of daily travel distance	94.42
Mean of daily travel distance	40
Maximum travel distance	400 km
Charging power (slow charging)	1.9 kW
Charging power (fast charging)	16 kW
Charging efficiency	90 %
Battery Capacity	80 kWh

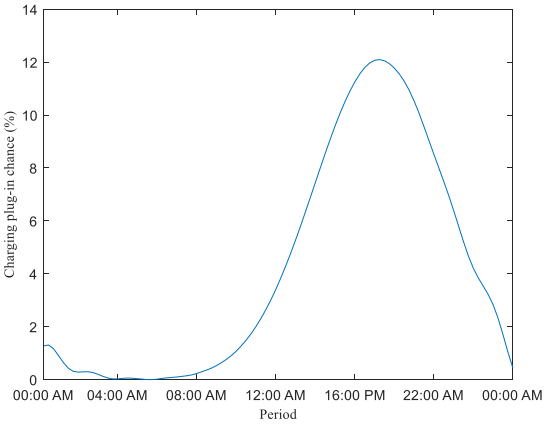

FIGURE 26. Plug-in time of home charger.

reduce the power loss of entire system by change load connection types that reduce between difference of the positive load demand and negative load demand. So, the neutral current of each bus and the system power loss are decreased.

FIGURE 22-25 presents the voltage profile of positive and negative poles. The simulation result shown that the optimal load connection can reduce the voltage drop of positive and negative pole of each bus. In positive pole, the lowest voltage magnitudes at bus 17 were improved to 0.967 p.u. for positive pole and -0.966 p.u. for negative pole and the VUF was reduced by 0.124% with the neutral voltage reduction to 1.27×10^{-3} p.u. In case of lowest voltage of negative pole that located at bus 18, a magnitude of positive pole and negative pole voltage were improved to 0.967 p.u. and -0.968 p.u, respectively. The neutral voltage at bus is 18 equal to -0.356×10^{-6} p.u. and the VUF of this bus is -0.006 %, which is changed in according to the difference of positive and negative voltage buses. So, the VUF improvement can reduce the neutral current flow of entire system that can

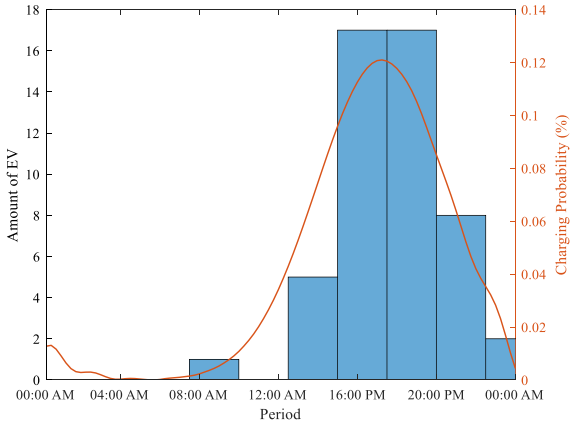

FIGURE 27. Total Plug-in time of home charger.

TABLE 7. MCS result on amount of EV at time interval.

Time interval	Amount of EV	Time interval	Amount of EV
07:30 AM-10:00 AM	1	17:30 PM-20:00 PM	17
12:30 PM-15:00 PM	5	20:00 PM-22:30 PM	8
15:00PM-17:30 PM	17	22:30 PM-00:00 AM	2

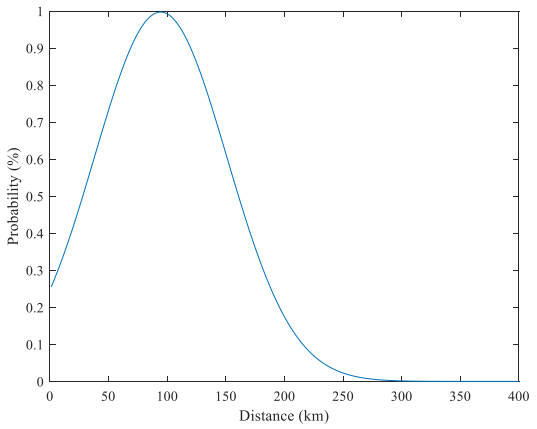

FIGURE 28. Probabilistic daily distance travel of EV.

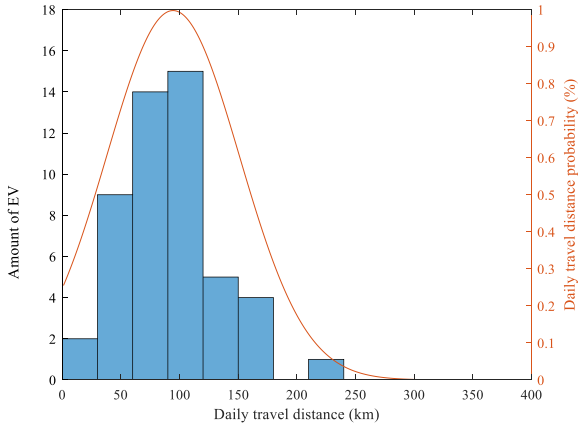

FIGURE 29. Probabilistic of daily distance travel.

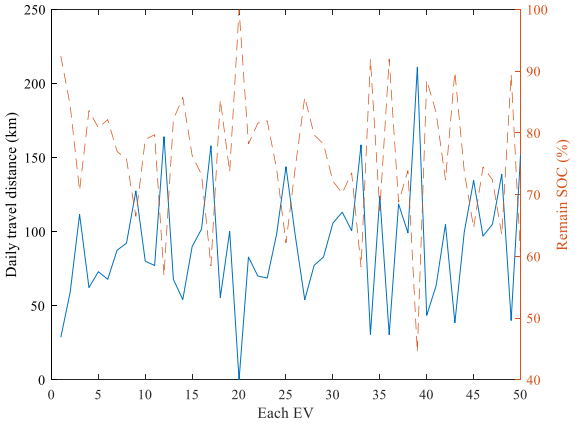

FIGURE 30. Remain SOC of each EV and daily distance travel.

TABLE 8. MCS result on total probabilistic daily distance of EVs.

Daily travel distance (km)	Amount of EV	Daily travel distance (km)	Amount of EV
0-30	2	121-150	5
31-60	9	151-180	4
61-90	14	181-210	0
91-120	15	211-240	1

reduce the power loss of the system by 50.821 % (from 958.100 kWh to 471.175 kWh), for this case.

C. PROBABILISTIC EV CHARGING MODELING

This subsection presents the MCS procedure for EV charging load which include probability of plug-in time and daily travel distance for random a sampling EV owner behavior. After that, the sampling data is used to calculate charging time and load demand. The condition of MCS simulation is given in TABLE 6

FIGURE 26 represents an EV charging behavior of home charger. Then, the total probabilistic plug-in time of EV owners' behavior can be obtained as shown in FIGURE 27 and TABLE 7.

FIGURE 27 presents the sampling data of EV charging at the times interval based on charging probability in TABLE 7. Consequently, the probability of daily distance travel that present the behavior of EV owners, can be calculated by using Equation 27. The result is shown in FIGURE 28.

FIGURE 28 present probability of daily distance travel of EV owner which varies from 0 km to 283 km. This probability function is used to obtain the daily travel distance for each EV. The result of total probabilistic daily distance travel is shown in FIGURE 29 and TABLE 8

The result in TABLE 8 presents a sampling data of daily distance travel of each EV. The simulation result is used to estimate remain SOC before charging. A number of EVs at

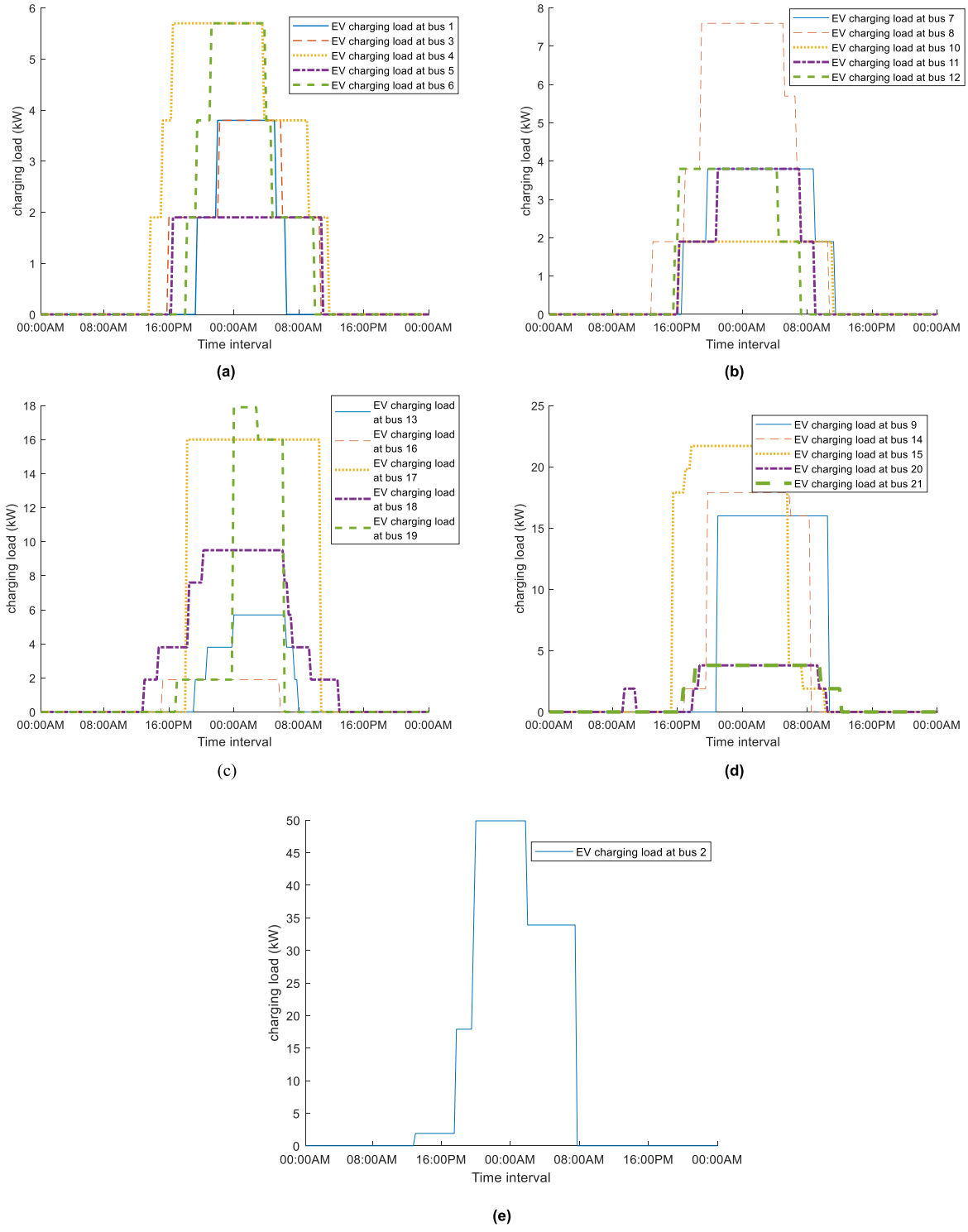

FIGURE 31. (a)-(e) EV home charging load pattern at every bus.

each bus can be random by using information in TABLE 8 and the result is shown in TABLE 9. Aforementioned, the result of remain SOCs and EV charging load demand can be shown in FIGURE 30.

FIGURE 30 presents the remaining of EV SOC sampling data based on PDF that related to daily travel distance. The simulation result is used to estimate the charging time of each EV.

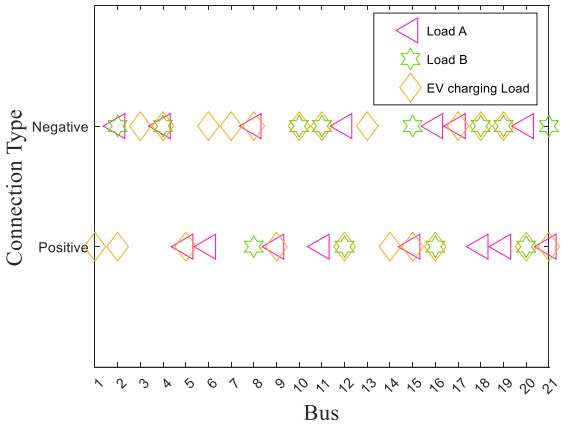

FIGURE 32. Load connection type of bipolar DC distribution grid.

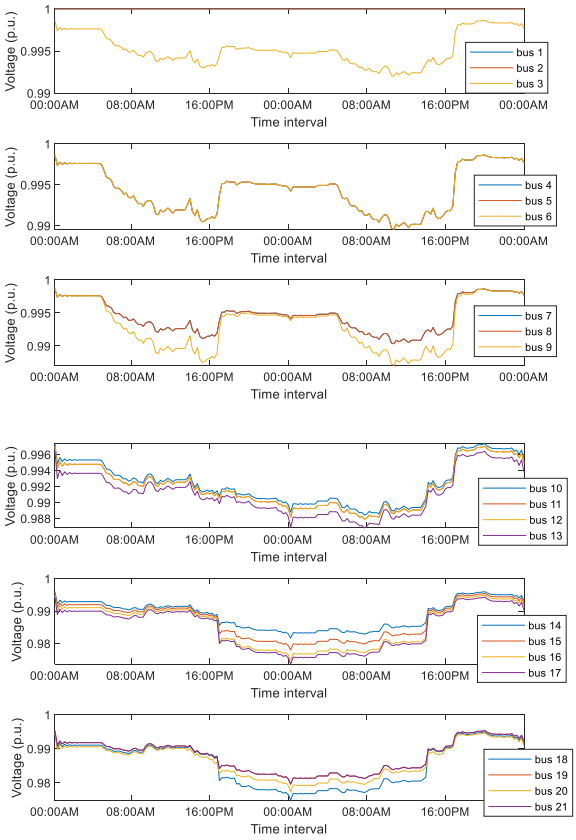

FIGURE 33. Positive voltage profile of case III.

FIGURE 31(a)-(e) present the EV load demand of every bus and amount of EV that charge at each bus in the system. The simulation result is used to calculate voltage profile at each bus and overall power loss in the next subsection.

D. PROBABILISTIC EV CHARGING LOAD CASE (CASE III)

This subsection presents the bipolar DCDG load flow with EV charging load integration based on EV load demand pattern from the previous section. The simulation result, including a voltage profile, power loss and VUF of entire system, are presented in FIGURES 32 –36.

TABLE 9. MCS result on the number of EVs connected at every buses.

Bus	Numbers of EVs	Bus	Numbers of EVs
1	2	12	2
2	4	13	3
3	2	14	2
4	3	15	4
5	1	16	1
6	3	17	1
7	2	18	5
8	4	19	2
9	1	20	3
10	1	21	2
11	2		

TABLE 10. The comparison of case II and case III.

Scenario	Highest VUF (%)	Total Daily Loss (kWh)
Case II	1.347 (Bus 12)	471.125
Case III	2.019 (Bus 17)	795.079

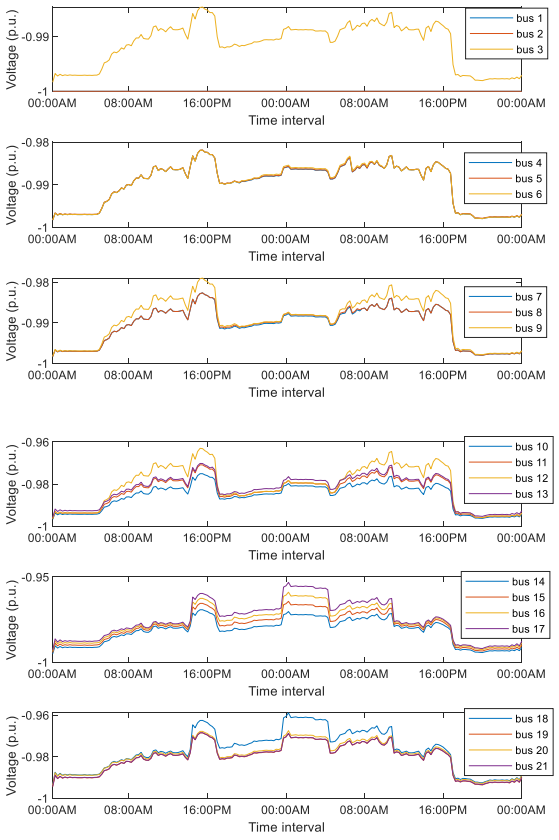

FIGURE 34. Negative voltage profile of case III.

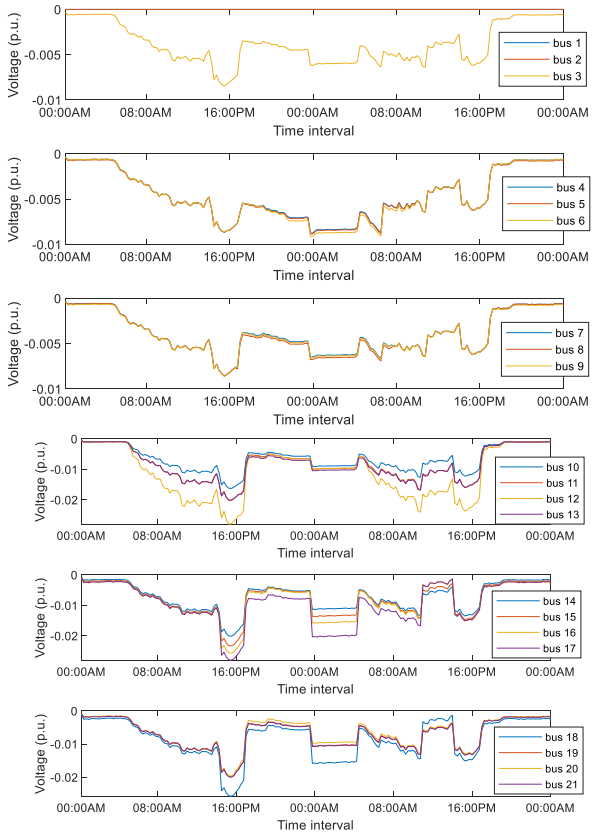

FIGURE 35. Neutral voltage profile of case III.

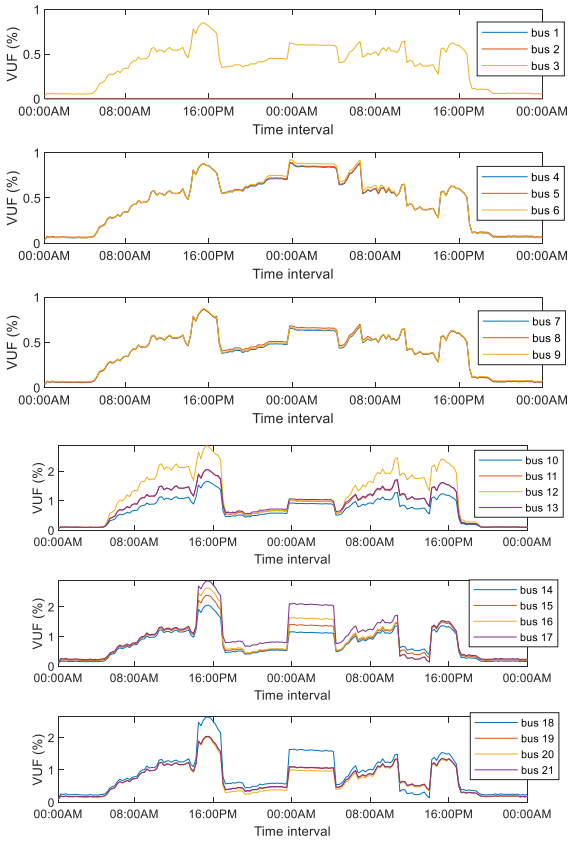

FIGURE 36. Voltage Unbalance Factor of case III.

FIGURE 32 presents a load connection type of load based on load balancing case (Case II) and the probability EV charging load case (Case III).

In this case, the lowest positive and lowest negative voltage magnitudes are at bus 17, in difference time interval. A lowest positive voltage magnitude is 0.962 p.u. at 09.15 a.m. or time slot 133 which caused by existing load and EV charging load. At bus 17, one EV connected to grid via charger with the power rated is 16 kW. The charging duration from 18.00 p.m. to 10.45 a.m. in the next day. So, the voltage drops of bus 17 are caused by the load demand of existing load and EV charging load. In case of negative pole on bus 17, The lowest voltage occurs at 00.15 a.m. or time slot 97, with negative and bipolar loads, without EV charging load. However, the negative voltage bus is reduced from 0.975 p.u. to 0.962 p.u. Therefore, the EV load demand can increase the power loss of entire system due to increasing current flow at each bus and create unbalance condition. The comparison result of Case II and Case III is shown in TABLE 10. From Table 10, it can be seen that the EV charging load can significantly increase the total power loss of the system by 68.76 %

E. PROBABILISTIC EV CHARGING LOAD WITH LOAD BALANCING CASE (CASE IV)

This subsection presents a load balancing with probabilistic EV load demand to mitigate the impact of EVs on DCDG

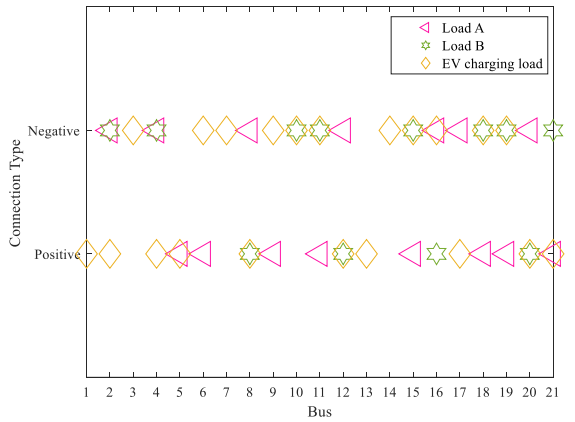

FIGURE 37. Load connection type of bipolar DC distribution grid.

by the proposed method. the optimal load connection types, solved by the proposed method is shown in FIGURE 37.

In the simulation results, the lowest voltage is at bus 17 for both poles. The lowest positive voltage magnitude is 0.948 p.u at bus 17 in 00.15 a.m., or time slot 97 and the lowest negative voltage magnitude is 0.957 p.u. in 09.15 a.m at bus 17, or time slot 133. Therefore, proposed method can reduce the VUF and total power loss of entire system by minimizing the difference of load demand between poles, and the neutral current flow between buses. A comparison of the

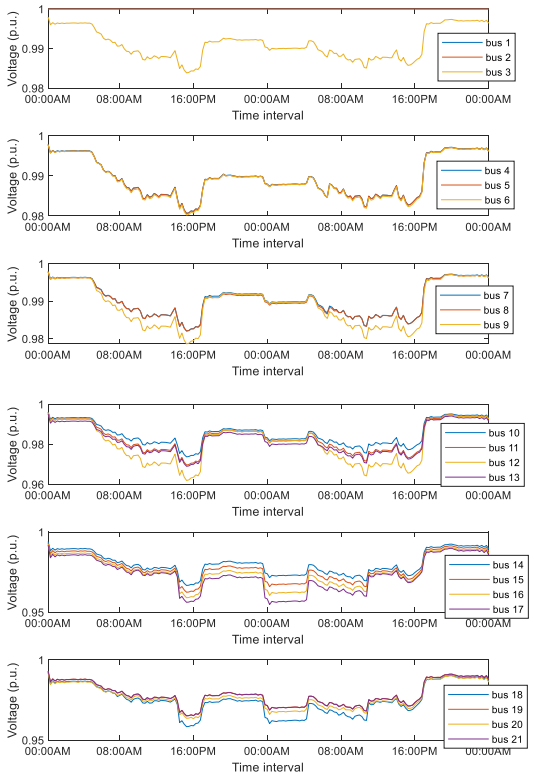

FIGURE 38. Positive voltage profile of case IV.

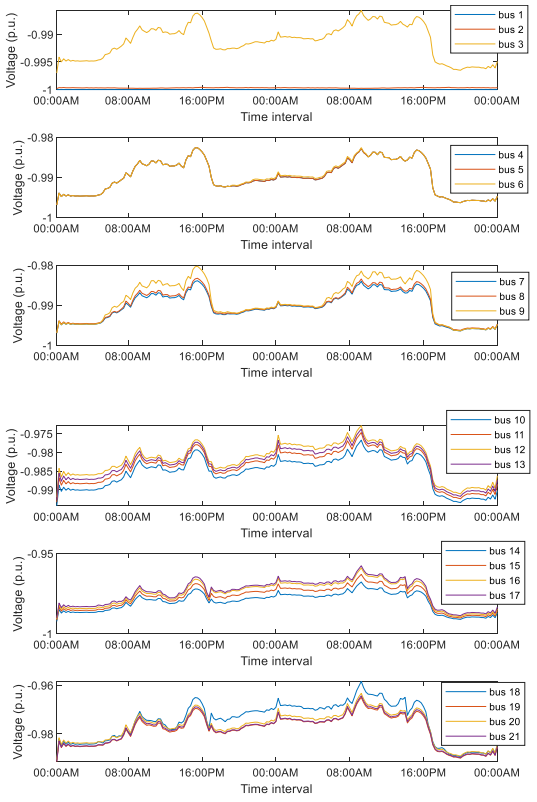

FIGURE 39. Negative voltage profile of case IV.

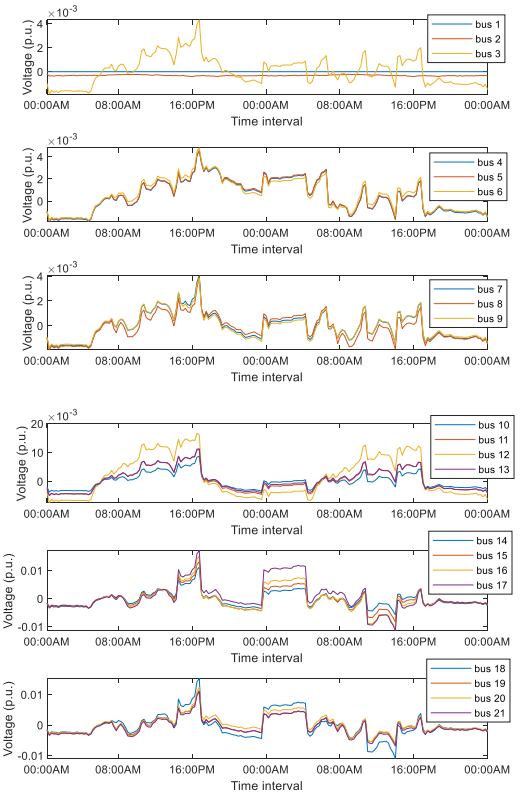

FIGURE 40. Neutral voltage profile of case IV.

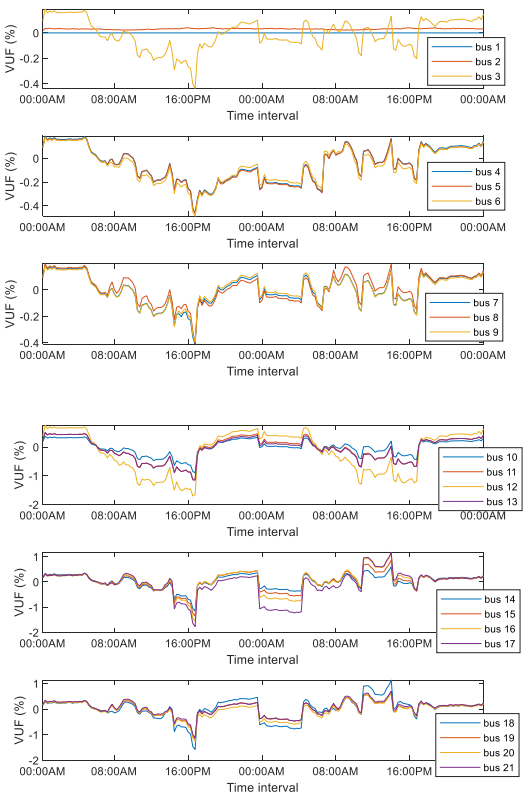

FIGURE 41. Voltage Unbalance Factor of case IV.

simulation results between case III and case IV is shown in TABLE 11. The optimal connection type of the case study can reduce total daily loss of entire system to 655.060 kWh or by 17.61%

TABLE 11. The comparison of Case III and Case IV For the highest VUF and total daily loss.

Scenario	Highest VUF (%)	Total daily loss (kWh)
Case III	5.379 (Bus 18)	795.079
Case IV	-1.766 (bus 17)	655.060

VIII. CONCLUSION

This paper investigated an impact of EV charging load on bipolar DCDG and proposed a method to improve the DCDG efficiency including mitigate the problem of EV charging load. The study includes the probabilistic model of EV charging load obtained by MCS to evaluate the charging demand during each time interval along the day. A DC power flow for bipolar DCDG, solved by GMM based Gauss's iteration method, is used to determine the voltage profile, VUF, and power loss of entire system. To minimize the total daily loss of DCDG by load balancing method, the optimal load connection type at each bus is searched by using PSO. The achievement of total daily loss minimization also leads to the reduction in VUF. The simulation results showed that the proposed load balancing method can significantly reduce the total daily loss and improve VUF of bipolar DGDC considering probabilistic EV charging load.

ACKNOWLEDGMENT

The authors would like to express their sincere gratitude to the Suranaree University of Technology (SUT), for providing the necessary support and resources for the completion of this research work. Their financial assistance and facilities have been instrumental in carrying out this study.

REFERENCES

[1] T. A. Edison, *System of Electrical Distribution*. NJ, USA: United State Patent Office, 1883.

[2] V. A. Prabhala, B. P. Baddipadiga, and M. Ferdowsi, "DC distribution systems—An overview," in *Proc. Int. Conf. Renew. Energy Res. Appl. (ICRERA)*, 2014, pp. 307–312.

[3] V. Nasirian, S. Moayedi, A. Davoudi, and F. L. Lewis, "Distributed cooperative control of DC microgrids," *IEEE Trans. Power Electron.*, vol. 30, no. 4, pp. 2288–2303, Apr. 2015.

[4] A. G. Anastasiadis, G. P. Kondylis, A. Polyzakis, and G. Vokas, "Effects of increased electric vehicles into a distribution network," *Energy Proc.*, vol. 157, pp. 586–593, Jan. 2019.

[5] G. A. Putrus, P. Suwanapingkarl, D. Johnston, E. C. Bentley, and M. Narayana, "Impact of electric vehicles on power distribution networks," in *Proc. IEEE Vehicle Power Propuls. Conf.*, Sep. 2009, pp. 827–831.

[6] Q. Tiantian, "Calculation of electric vehicle charging power based on spatial–temporal activity model," in *Proc. China Int. Conf. Electr. Distrib. (CICED)*, Sep. 2018, pp. 2884–2888.

[7] C. Camus, C. M. Silva, T. L. Farias, and J. Esteves, "Impact of plug-in hybrid electric vehicles in the Portuguese electric utility system," in *Proc. Int. Conf. Power Eng., Energy Electr. Drives*, Mar. 2009, pp. 285–290.

[8] S. Schey, D. Scoffield, and J. Smart, "A first look at the impact of electric vehicle charging on the electric grid in the EV project," *World Electr. Vehicle J.*, vol. 5, no. 3, pp. 667–678, Sep. 2012.

[9] P. Morrissey, P. Weldon, and M. O'Mahony, "Future standard and fast charging infrastructure planning: An analysis of electric vehicle charging behaviour," *Energy Policy*, vol. 89, pp. 257–270, Feb. 2016.

[10] D. Kumar, F. Zare, and A. Ghosh, "DC microgrid technology: System architectures, AC grid interfaces, grounding schemes, power quality, communication networks, applications, and standardizations aspects," *IEEE Access*, vol. 5, pp. 12230–12256, 2017.

[11] A. de Almeida, P. Moura, and N. Quaresma, "Energy-efficient off-grid systems—Review," *Energy Efficiency*, vol. 13, no. 2, pp. 349–376, Feb. 2020.

[12] F. Wang, L. Wang, X. Zhang, J. Wang, S. Li, and Y. Liu, "Voltage level study for DC distribution grid based on comprehensive evaluation," in *Proc. IEEE Int. Conf. Power Electron., Comput. Appl. (ICPECA)*, Jan. 2021, pp. 492–496.

[13] T. Kaipia, P. Nuutinen, A. Pinomaa, A. Lana, J. Partanen, J. Lohjala, and M. Matikainen, "Field test environment for LVDC distribution—Implementation experiences," in *Proc. CIRED Workshop, Integr. Renewables Distrib. Grid*, May 2012, pp. 1–4.

[14] E. Rodriguez-Diaz, F. Chen, J. C. Vasquez, J. M. Guerrero, R. Burgos, and D. Boroyevich, "Voltage-level selection of future two-level LVdc distribution grids: A compromise between grid compatibiliy, safety, and efficiency," *IEEE Electrific. Mag.*, vol. 4, no. 2, pp. 20–28, Jun. 2016.

[15] Y. Yoldaş, A. Önen, S. M. Muyeen, A. V. Vasilakos, and İ. Alan, "Enhancing smart grid with microgrids: Challenges and opportunities," *Renew. Sustain. Energy Rev.*, vol. 72, pp. 205–214, May 2017.

[16] A. Jhunjhunwala, A. Lolla, and P. Kaur, "Solar-DC microgrid for Indian homes: A transforming power scenario," *IEEE Electrific. Mag.*, vol. 4, no. 2, pp. 10–19, Jun. 2016.

[17] J. Karppanen, T. Kaipia, P. Nuutinen, A. Lana, P. Peltoniemi, A. Pinomaa, A. Mattsson, J. Partanen, J. Cho, and J. Kim, "Effect of voltage level selection on earthing and protection of LVDC distribution systems," in *Proc. 11th IET Int. Conf. AC DC Power Transmiss.*, Feb. 2015, pp. 1–8.

[18] H. Kakigano, Y. Miura, T. Ise, and R. Uchida, "DC voltage control of the DC micro-grid for super high quality distribution," in *Proc. Power Convers. Conf. Nagoya*, Apr. 2007, pp. 518–525.

[19] G. Sakulphaisan and K. Chayakulkheeree, "Improve a voltage unbalance index of bipolar DC distribution grid by using particle swarm optimization based on load balancing method," in *Proc. Int. Electr. Eng. Congr. (iEECON)*, Mar. 2022, pp. 1–4.

[20] S. Anand, B. G. Fernandes, and J. Guerrero, "Distributed control to ensure proportional load sharing and improve voltage regulation in low-voltage DC microgrids," *IEEE Trans. Power Electron.*, vol. 28, no. 4, pp. 1900–1913, Apr. 2013.

[21] I. Sharma, C. Cañizares, and K. Bhattacharya, "Smart charging of PEVs penetrating into residential distribution systems," *IEEE Trans. Smart Grid*, vol. 5, no. 3, pp. 1196–1209, May 2014.

[22] A. Chiş, J. Rajasekharan, J. Lundén, and V. Koivunen, "Demand response for renewable energy integration and load balancing in smart grid communities," in *Proc. 24th Eur. Signal Process. Conf. (EUSIPCO)*, Aug. 2016, pp. 1423–1427.

[23] J. Kennedy and R. Eberhart, "Particle swarm optimization," in *Proc. Int. Conf. Neural Netw. (ICNN)*, vol. 4, 1995, pp. 1942–1948.

[24] R. A. Verzijlbergh, M. O. W. Grond, Z. Lukszo, J. G. Slootweg, and M. D. Ilic, "Network impacts and cost savings of controlled EV charging," *IEEE Trans. Smart Grid*, vol. 3, no. 3, pp. 1203–1212, Sep. 2012.

[25] G. Saldaña, J. I. S. Martin, I. Zamora, F. J. Asensio, and O. Oñederra, "Electric vehicle into the grid: Charging methodologies aimed at providing ancillary services considering battery degradation," *Energies*, vol. 12, no. 12, p. 2443, Jun. 2019, doi: 10.3390/en12122443.

[26] M. Gilleran, E. Bonnema, J. Woods, P. Mishra, I. Doebber, C. Hunter, M. Mitchell, and M. Mann, "Impact of electric vehicle charging on the power demand of retail buildings," *Adv. Appl. Energy*, vol. 4, Nov. 2021, Art. no. 100062.

[27] S. Deilami, A. S. Masoum, P. S. Moses, and M. A. S. Masoum, "Real-time coordination of plug-in electric vehicle charging in smart grids to minimize power losses and improve voltage profile," *IEEE Trans. Smart Grid*, vol. 2, no. 3, pp. 456–467, Sep. 2011.

[28] N. I. Nimalsiri, C. P. Mediwaththe, E. L. Ratnam, M. Shaw, D. B. Smith, and S. K. Halgamuge, "A survey of algorithms for distributed charging control of electric vehicles in smart grid," *IEEE Trans. Intell. Transp. Syst.*, vol. 21, no. 11, pp. 4497–4515, Nov. 2020.

[29] S. Alshahrani, M. Khalid, and M. Almuhaini, "Electric vehicles beyond energy storage and modern power networks: Challenges and applications," *IEEE Access*, vol. 7, pp. 99031–99064, 2019.
[30] A. H. Einaddin and A. S. Yazdankhah, "A novel approach for multi-objective optimal scheduling of large-scale EV fleets in a smart distribution grid considering realistic and stochastic modeling framework," *Int. J. Electr. Power Energy Syst.*, vol. 117, May 2020, Art. no. 105617.
[31] K. Clement-Nyns, E. Haesen, and J. Driesen, "The impact of charging plug-in hybrid electric vehicles on a residential distribution grid," *IEEE Trans. Power Syst.*, vol. 25, no. 1, pp. 371–380, Feb. 2010.
[32] E. Sortomme, M. M. Hindi, S. D. J. MacPherson, and S. S. Venkata, "Coordinated charging of plug-in hybrid electric vehicles to minimize distribution system losses," *IEEE Trans. Smart Grid*, vol. 2, no. 1, pp. 198–205, Mar. 2011.
[33] S. Aghajan-Eshkevari, S. Azad, M. Nazari-Heris, M. T. Ameli, and S. Asadi, "Charging and discharging of electric vehicles in power systems: An updated and detailed review of methods, control structures, objectives, and optimization methodologies," *Sustainability*, vol. 14, no. 4, p. 2137, Feb. 2022, doi: 10.3390/su14042137.
[34] S. Bahrami and M. Parniani, "Game theoretic based charging strategy for plug-in hybrid electric vehicles," *IEEE Trans. Smart Grid*, vol. 5, no. 5, pp. 2368–2375, Sep. 2014.
[35] S. S. Amiri, S. Jadid, and H. Saboori, "Multi-objective optimum charging management of electric vehicles through battery swapping stations," *Energy*, vol. 165, pp. 549–562, Dec. 2018.
[36] K. Zhou, L. Cheng, L. Wen, X. Lu, and T. Ding, "A coordinated charging scheduling method for electric vehicles considering different charging demands," *Energy*, vol. 213, Dec. 2020, Art. no. 118882.
[37] B. S. H. Chew, Y. Xu, and Q. Wu, "Voltage balancing for bipolar DC distribution grids: A power flow based binary integer multi-objective optimization approach," *IEEE Trans. Power Syst.*, vol. 34, no. 1, pp. 28–39, Jan. 2019.

GUNTINAN SAKULPHAISAN (Graduate Student Member, IEEE) was born in Chaiyaphum, Thailand, in 1995. He received the bachelor's and master's degrees in electrical engineering from the Suranaree University of Technology (SUT), in 2017 and 2019, respectively, where he is currently pursuing the Ph.D. degree in electrical engineering. His research interests include electric vehicles (EV), dc grid, and railway electrification.

KEERATI CHAYAKULKHEEREE (Senior Member, IEEE) received the B.Eng. degree in EE from KMITL, in 1995, and the M.Eng. and D.Eng. degrees in electric power system management from AIT, in 1999 and 2004, respectively. He is currently an Associate Professor with the School of Electrical Engineering, Institute of Engineering, Suranaree University of Technology, Thailand.